

Si clusters on reconstructed SiC (0001) revealed by surface extended x-ray absorption fine structure

Xingyu Gao,^{1,a)} Shi Chen,¹ Tao Liu,¹ Wei Chen,¹ A. T. S. Wee,¹ T. Nomoto,² S. Yagi,² Kazuo Soda,² and Junji Yuhara³

¹Department of Physics, National University of Singapore, 2 Science Drive 3, Singapore 117542, Singapore

²Department of Materials, Physics and Energy Engineering, Nagoya University, Nagoya 464-8603, Japan

³Department of Physical Science and Engineering, School of Engineering, Nagoya University, Nagoya 464-8603, Japan

(Received 11 May 2009; accepted 10 September 2009; published online 6 October 2009)

The evolution of silicon carbide (0001) surface reconstruction upon annealing has been studied by Si *K* edge extended x-ray absorption fine structure (EXAFS). Using Si *KVV* Auger electron yield at different emission angles with different surface sensitivities, EXAFS reveals conclusively that Si–Si bonds exist on the surface for all reconstructions. The existence of Si clusters on the $6\sqrt{3} \times 6\sqrt{3}R30^\circ$ surface was also confirmed by x-ray photoemission spectroscopy. This finding gives us a better understanding of epitaxial graphene formation on SiC. © 2009 American Institute of Physics. [doi:10.1063/1.3242005]

Graphene has generated much interest recently with the prospect of graphene-based nanometer-scale electronics.^{1,2} Epitaxial graphene (EG) is formed upon annealing SiC at 1200–1300 °C after a series of surface reconstructions.³ Different surface reconstructions were found for SiC which depend on the polytype, surface termination as well as surface preparation conditions.⁴ In particular, Si terminated 6H-SiC(0001) surfaces evolve through a series of reconstructions from 3×3 , to $\sqrt{3} \times \sqrt{3}R30^\circ$, to $6\sqrt{3} \times 6\sqrt{3}R30^\circ$ and finally to EG upon annealing.^{5–10} The understanding of this evolution as well as the atomic structure of each reconstruction, especially the $6\sqrt{3} \times 6\sqrt{3}R30^\circ$, is crucial to fully understand the structure and the properties of EG for its applications. Many experimental^{5–10} and theoretical efforts^{11,12} have been devoted to studying the atomic arrangements of these surface reconstructions. The starting 3×3 reconstruction is currently most accurately described by the model proposed by Starke *et al.*,¹³ which describes a silicon tetramer on a twisted Si adlayer with clover-like rings. For the $\sqrt{3} \times \sqrt{3}R30^\circ$ reconstruction, theoretical *ab initio* calculations¹⁴ show the Si atom in the T4 site, and this conclusion is further supported by grazing-incidence x-ray diffraction and photoelectron diffraction experiments.^{15,16} Despite much effort, the $6\sqrt{3} \times 6\sqrt{3}R30^\circ$ reconstruction remains the most controversial. It was proposed that this reconstruction arises from an incommensurate graphite overlayer.¹⁷ An x-ray photoemission spectroscopy (XPS) study by Johansson *et al.*¹⁸ suggested that this reconstruction could be attributed to carbon in a Si-deficient environment without surface graphitization. Owman and Martensson¹⁹ explained the $6\sqrt{3} \times 6\sqrt{3}R30^\circ$ reconstruction observed by diffraction as a mixture of $\sqrt{3} \times \sqrt{3}R30^\circ$, 6×6 , and 5×5 domains from their STM study. A combined STM and XPS study by Ong and Tok²⁰ reports that the evolution of SiC upon annealing follows 3×3 , Si rich 6×6 clusters at 1000 °C and 6×6 rings at 1100 °C, at the temperature $6\sqrt{3} \times 6\sqrt{3}R30^\circ$ is believed to exist.

From all these studies of SiC reconstructions, Si is shown to play a vital role even in the $6\sqrt{3} \times 6\sqrt{3}R30^\circ$ reconstruction. It is therefore useful to investigate the Si local arrangement and chemical properties. Previously we reported the evolution of Si *K* edge near edge x-ray absorption fine structure to show an increasing number of Si vacancies due to the outdiffusion of Si atoms at high temperature annealing.²¹ Extended x-ray absorption fine structure (EXAFS), on the other hand, reveals element-specific quantitative local structural information. As x-ray absorption spectra (XAS) can be measured using different signal sources, its probe depth can be varied for depth-dependent information.²² In this study, we use Si *KVV* Auger electron yield at different emission angles for the measurement of Si *K* edge XAS. For Si *KVV* Auger electrons with kinetic energy of 1850 eV, the mean free path is about 3.7 nm.²³ Using grazing emission angles, even more surface sensitive information can also be obtained.

The experiments were carried out at the double crystal monochromator beamline (BL-3) at HiSOR.²⁴ The samples were cut from N-doped *n*-type 6H-SiC(0001) single crystal wafers with dopant concentration of 10^{18} cm^{-3} from CREE Research. The Si *K*-edge XAS measurements were performed using Si *KVV* Auger electron yield detected by an electron analyzer at both normal (0°) and 70° grazing emission angles. The details about the sample preparation and experimental setup can be found elsewhere.²¹ To compare with the experimental data, Si *K*-edge EXAFS calculations were carried out using the FEFF8 code (version 8.20, University of Washington).²⁵ As there are three nonequivalent crystallographic sites of Si in the 6H-SiC unit cell,²⁶ the calculated EXAFS was performed for all Si atoms and averaged over the three sites.

As reported previously, XAS using fluorescence yield deviates greatly from the real absorption cross section due to the strong saturation effects.²¹ Therefore, we used Auger yield to measure EXAFS spectra. Although measurement was made on EG, no reasonable spectrum was obtained due to the fact that Si Auger electrons are too surface sensitive

^{a)}Electronic mail: phygaoxy@nus.edu.sg.

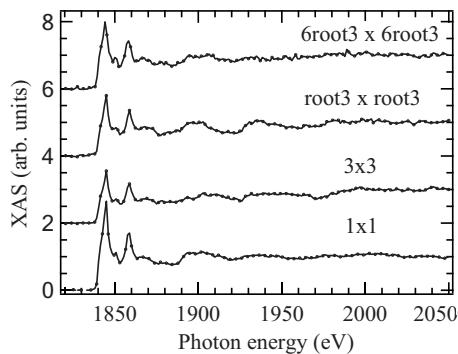


FIG. 1. Si K EXAFS spectra for different SiC surfaces measured using Si KVV Auger electron yield at a grazing angle of 70° .

for this C-terminated surface to deliver enough count rates. Figure 1 reports the Si K edge EXAFS spectra for different SiC surface structures measured using Si KVV Auger electron yield at the surface sensitive grazing angle of 70° . The near edge spectra of Si K edges are consistent with previous reports.^{21,27,28} In the extended region, distinct oscillations are observed for the different surface reconstructions.

The Fourier transform of the measured EXAFS spectra after k^3 weighting using WINXAS are presented in Fig. 2. The local structural changes around Si atoms upon annealing for different surface reconstructions are clearly resolved. For a better understanding, theoretical curves using FEFF are also shown for both 6H-SiC and Si in Fig. 2. The first peak in the calculated curve of 6H-SiC corresponds to the first Si-C coordination at 1.4 \AA , and the second peak at 2.4 \AA is from the Si-Si coordination. In the case of Si which has a diamond-like structure, the first peak of Si-Si coordination is calculated at about 1.9 \AA and the second peak for the next nearest neighbor at 3.4 \AA . The calculated curves are consistent with

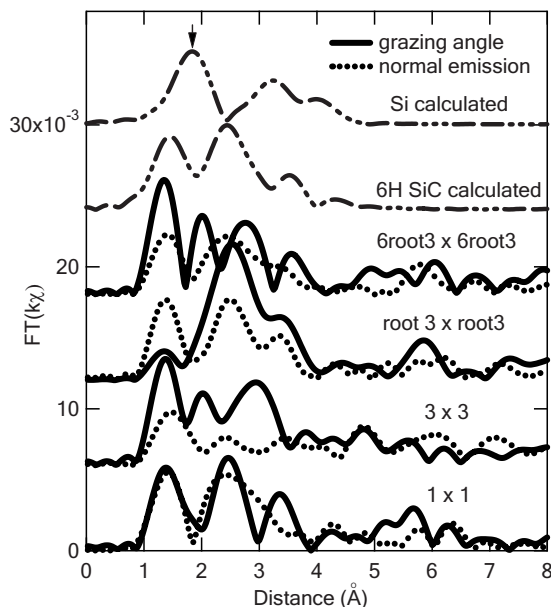


FIG. 2. Fourier transforms (not corrected for phase-shift) of the Si K edge EXAFS data for different SiC surface structures measured by using Auger yield at both normal emission (dashed lines) and an emission angle of 70° (solid lines). For comparison, theoretical calculated curves for 6H-SiC and Si are also present. The curves from the bottom to the top are 1×1 , 3×3 , $\sqrt{3} \times \sqrt{3}R30^\circ$, and $6\sqrt{3} \times 6\sqrt{3}R30^\circ$, calculated 6H-SiC, and Si, respectively. The arrow indicates the first coordination of Si atom in Si lattice.

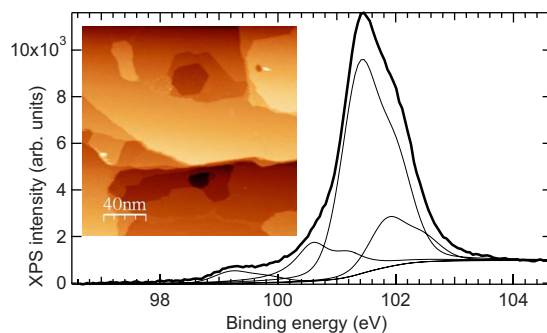


FIG. 3. (Color online) Si $2p$ XPS spectrum from $6\sqrt{3} \times 6\sqrt{3}R30^\circ$ surface. The thin lines represent the fitting results and the inset is an STM image of this surface.

the experimental data in the literature.^{28–30} Now we turn to the experimental results. For the primitive 1×1 surface, the first two peaks for normal emission and grazing emission are at the same locations with the calculated 6H-SiC phase. For the 3×3 reconstruction, it is clear that the curve at normal emission has its first two peaks located at the same positions as the primitive surface in Fig. 2. However, the curve at grazing emission angle looks quite different: although the first peak remains at 1.4 \AA , the second peak is located at about 2 \AA . Comparing to the theoretical calculation, the second peak is attributed to Si-Si coordination on the surface due to the high surface sensitivity at grazing emission angle. Our EXAFS results thus indicate the existence of Si clusters on this reconstructed surface. This is consistent with the Starke model where Si tetramers form atop the surface.¹³ As the 3×3 reconstruction was obtained by Si dosage at high temperature, it is reasonable that Si clusters form on the surface.^{13,20} For the $\sqrt{3} \times \sqrt{3}R30^\circ$ reconstruction, the normal emission curve is almost identical to the calculated one for 6H-SiC due to the deeper probing. For the curve measured at grazing angle, the first peak is weak and the second peak become much broader and centered at 2.5 \AA . This suggests that the coordination of Si atoms on this reconstruction is more complicated. There could be Si-Si bonds formed on the surface with different bond lengths and different phase shifts, which causes the first peak of the Si cluster to almost vanish and merge with the second peak of primitive 6H-SiC. This observation is consistent with the report by Ong and Tok,²⁰ where Si clusters exist in several different types of clusters between 1000° and 1100° . For the $6\sqrt{3} \times 6\sqrt{3}R30^\circ$ reconstruction, the curve for normal emission still resembles the SiC phase. However, for the curve measured at grazing angle, the peak corresponding to Si-Si coordination at 2 \AA from Si clusters is very clearly resolved beside the first peak corresponding to the Si-C coordination. As the probing depth of AEY at normal emission is 3.7 nm and that at 70° reduced to 1.3 nm , it can be concluded that Si clusters should remain on this reconstructed surface even though the surface is no longer Si rich. This finding supports the results by Ong and Tok,²⁰ where they proposed Si clusters formed on top of the surface with underlying C atoms exposed in some regions.

To confirm the existence of Si clusters on the $6\sqrt{3} \times 6\sqrt{3}R30^\circ$ surface, Fig. 3 shows the Si $2p$ XPS spectrum from this surface at normal emission angle, which was measured at the SINS beamline at the Singapore Synchrotron Light Source using photon energy of 140 eV .³¹ The inset

shows a scanning tunneling microscopy (STM) image measured on the same sample which shows no observable Si crystallites. Fitting analysis of the XPS spectrum reveals two components at 99.2 eV and 100.6 eV besides two other bulk components at higher binding energies, which is consistent with previous report of two Si surface components.¹⁸ The component at 99.2 eV is close to the binding energy of elemental Si, the one at 100.6 eV could thus have both Si–Si and Si–C bonds. It is noticed that these two surface components accounts for 4.5% and 10.4% of total intensity, respectively, which gives a ratio between them of about 1:2.3. This suggests that the Si clusters could consist of a Si center atoms on top of three corner Si atoms with photoemission from the bottom three atoms be attenuated by the top atom, which is consistent with Si₄ clusters proposed in Ref. 20. Thus, the center Si atom has only Si–Si bonds whereas the corner Si atoms have both Si–Si bonds and Si–C bonds. As the two surface components accounts for about 15% of total intensity, we can roughly estimate that Si clusters formed on $6\sqrt{3} \times 6\sqrt{3}R30^\circ$ surface covers only about 10% of the surface.

As we reported previously, Si vacancies form in much deeper layers due to the outdiffusion of Si.²¹ These outdiffused Si atoms must contribute to the formation of Si clusters on the surface, especially for the $6\sqrt{3} \times 6\sqrt{3}R30^\circ$ reconstructed C rich surface. At around 1200–1300 °C when EG is formed, Si atoms will continue to outdiffuse from the bulk. However, most of them reach the surface and desorb without forming detectable Si clusters on the surface. A recent study³² on Si-terminated 4H- and 6H-SiC(0001) showed that the phase transition temperatures between different reconstructions can be varied over a wide temperature range by establishing thermodynamic equilibrium between the SiC sample and the external Si vapor pressure, which emphasizes the importance of the steady state Si concentration. A detailed study of Si outdiffusion, segregation, desorption should give a full picture of the mechanism of SiC reconstructions including EG formation, which is vital for the applications of EG.

In conclusion, Si *K* edge EXAFS conclusively shows that Si clusters exists in the surface region for all the reconstructed 6H-SiC surfaces, including the C-rich $6\sqrt{3} \times 6\sqrt{3}R30^\circ$ reconstruction, which acts as the buffer or interfacial layer in EG formation on SiC.³³ The outdiffusion of Si atoms from the interior of SiC contributes to these clusters. This information is critical to understanding the mechanism of SiC(0001) surface reconstructions including EG formation.

The authors acknowledge the financial support from A*STAR and JSPS Bilateral Joint Projects and NRF CRP Grant No. R-143-000-360-281 for the present research work.

- ¹A. Mattausch and O. Pankratov, *Phys. Rev. Lett.* **99**, 076802 (2007).
- ²S. Y. Zhou, G.-H. Gweon, A. V. Fedorov, P. N. First, W. A. De Heer, D.-H. Lee, F. Guinea, A. H. Castro Neto, and A. Lanzara, *Nature Mater.* **6**, 770 (2007).
- ³W. Chen, H. Xu, L. Liu, X. Y. Gao, D. C. Qi, G. W. Peng, S. C. Tan, Y. P. Feng, K. P. Loh, and A. T. S. Wee, *Surf. Sci.* **596**, 176 (2005).
- ⁴J. Pollmann and P. Krüger, *J. Phys.: Condens. Matter* **16**, S1659 (2004).
- ⁵V. M. Bermudez, *Appl. Surf. Sci.* **84**, 45 (1995).
- ⁶V. van Elsbergen, T. U. Kampen, and W. Monch, *Surf. Sci.* **365**, 443 (1996).
- ⁷T. Tsukamoto, M. Hirai, M. Kusaka, M. Iwami, T. Ozawa, T. Nagamura, and T. Nakata, *Surf. Sci.* **371**, 316 (1997).
- ⁸I. Forbeaux, J. M. Themlin, V. Langlais, L. M. Yu, H. Belkhir, and J. M. Debever, *Surf. Rev. Lett.* **5**, 193 (1998).
- ⁹X. N. Xie, H. Q. Wang, A. T. S. Wee, and K. P. Loh, *Surf. Sci.* **478**, 57 (2001).
- ¹⁰M. Naitoh, J. Takami, S. Nishigaki, and N. Toyama, *Appl. Phys. Lett.* **75**, 650 (1999).
- ¹¹P. Badziag, *Surf. Sci.* **337**, 1 (1995).
- ¹²M. Rohlfing and J. Pollman, *Phys. Rev. Lett.* **84**, 135 (2000).
- ¹³U. Starke, J. Schardt, J. Bernhardt, M. Franke, K. Reuter, H. Wedler, K. Heinz, J. Furthmüller, P. Käckell, and F. Bechstedt, *Phys. Rev. Lett.* **80**, 758 (1998); J. Schardt, J. Bernhardt, U. Starke, and K. Heinz, *Phys. Rev. B* **62**, 10335 (2000).
- ¹⁴J. E. Northrup and J. Neugebauer, *Phys. Rev. B* **52**, R17001 (1995); M. Sabisch, P. Kruger, and J. Pollmann, *ibid.* **55**, 10561 (1997).
- ¹⁵A. Coati, M. S. Simkin, Y. Garreau, R. Pinchaux, T. Argunova, and K. Aid, *Phys. Rev. B* **59**, 12224 (1999).
- ¹⁶G. Zampieri, S. Lizzit, L. Petaccia, and A. Goldoni, *Phys. Rev. B* **72**, 165327 (2005).
- ¹⁷M. H. Tsai, C. S. Chang, J. D. Dow, and I. S. T. Tsong, *Phys. Rev. B* **45**, 1327 (1992); L. Li and I. S. T. Tsong, *Surf. Sci.* **351**, 141 (1996).
- ¹⁸L. I. Johansson, F. Owman, and P. Martensson, *Phys. Rev. B* **53**, 13793 (1996).
- ¹⁹F. Owman and P. Martensson, *Surf. Sci.* **330**, L639 (1995).
- ²⁰W. J. Ong and E. S. Tok, *Phys. Rev. B* **73**, 045330 (2006).
- ²¹X. Y. Gao, S. Chen, T. Liu, W. Chen, A. T. S. Wee, T. Nomoto, S. Yagi, K. Soda, and J. Yuhara, *Phys. Rev. B* **78**, 201404 (2008).
- ²²X. Y. Gao, H. Xu, A. T. S. Wee, W. Kuch, C. Tieg, and S. Wang, *J. Appl. Phys.* **97**, 103527 (2005).
- ²³M. Krawczyk, L. Zommer, A. Kosinski, J. W. Sobczak, and A. Jablonski, *Surf. Interface Anal.* **38**, 644 (2006).
- ²⁴S. Yagi, G. Kutluk, T. Matsui, A. Matano, A. Hiraya, E. Hashimoto, and M. Taniguchi, *Nucl. Instrum. Methods Phys. Res. A* **467–468**, 723 (2001).
- ²⁵A. L. Ankudinov, B. Ravel, J. J. Rehr, and S. D. Conradson, *Phys. Rev. B* **58**, 7565 (1998).
- ²⁶A. H. Gomes de Mesquita, *Acta Crystallogr.* **1**, 1948 (1967).
- ²⁷Y. Baba, T. Sekiguchi, I. Shimoyama, and G. Krishna Nath, *Appl. Surf. Sci.* **237**, 176 (2004).
- ²⁸Y. H. Tang, T. K. Sham, D. Yang, and L. Xue, *Appl. Surf. Sci.* **252**, 3386 (2006).
- ²⁹A. M. Haghiri-Gosnet, F. Rousseaux, E. Gat, J. Durand, and A. M. Flank, *Microelectron. Eng.* **17**, 215 (1992).
- ³⁰C. J. Glover, G. J. Foran, and M. C. Ridgway, *Nucl. Instrum. Methods Phys. Res. B* **199**, 195 (2003).
- ³¹X. J. Yu, O. Wilhelmi, H. O. Moser, S. V. Vidyaraj, X. Gao, A. T. S. Wee, T. Nyunt, H. Qian, and H. Zheng, *J. Electron Spectrosc. Relat. Phenom.* **144–147**, 1031 (2005).
- ³²R. M. Tromp and J. B. Hannon, *Phys. Rev. Lett.* **102**, 106104 (2009).
- ³³S. W. Poon, W. Chen, E. S. Tok, and A. T. S. Wee, *Appl. Phys. Lett.* **92**, 104102 (2008).